Investigation of candidate genes and mechanisms underlying postmenopausal osteoporosis using bioinformatics analysis

XIAOZHONG ZHU, ZHIYUAN WANG, YANXUN ZHAO and CHAO JIANG

Department of Orthopedic Surgery, Tongji Hospital, Tongji University, Shanghai 200065, P.R. China

Received June 29, 2017; Accepted October 6, 2017

DOI: 10.3892/mmr.2017.8045

Abstract. The present study aimed to determine candidate genes, chemicals and mechanisms underlying postmenopausal osteoporosis (PMOP). A gene expression profile (accession no. GSE68303), which included 12 tissue samples from ovariectomized mice (OVX group) and 11 normal tissue samples from sham surgery mice (control group), was downloaded from the Gene Expression Omnibus database. The identification of differentially expressed genes (DEGs), and Gene Ontology functional enrichment and Kyoto Encyclopedia of Genes and Genomes pathway analyses, was performed, followed by an investigation of protein-protein interactions (PPI), PPI modules, transcription factors (TFs) and chemicals. A total of 784 upregulated and 729 downregulated DEGs between the two groups were identified. Furthermore, 2 upregulated modules and 6 downregulated modules were determined. The upregulated DEGs in modules were enriched in 'sensory perception of smell' function and 'olfactory transduction' pathway, and a number of genes belonging to the olfactory receptor (OLFR) family were identified in upregulated modules. The downregulated DEGs in modules were enriched in 'DNA replication initiation' function and 'cell cycle' pathway. A total of 8 TFs, including SP1 TF (SP1) and protein C-ets-1 (ETS1), were associated with PMOP. Furthermore, estradiol and resveratrol were identified as key chemicals in the chemical-gene interaction network. Therefore, TFs, including SP1 and ETS1, in addition to members of the OLFR gene family, may be employed as novel targets for treatment of PMOP. Furthermore, functions including 'sensory perception of smell' and 'replication initiation', and 'olfactory transduction' and 'cell cycle' pathways, may serve roles in PMOP. In addition, based on the chemical-gene interaction network, estradiol and resveratrol may also be considered for the treatment PMOP.

Correspondence to: Dr Xiaozhong Zhu, Department of Orthopedic Surgery, Tongji Hospital, Tongji University, 389 Xincun Road, Shanghai 200065, P.R. China
E-mail: zhuxiaozhong1716@126.com

Key words: postmenopausal osteoporosis, differentially expressed gene, pathway, protein-protein interaction network, transcriptional regulatory network, chemical-gene regulatory network

Introduction

Postmenopausal osteoporosis (PMOP) is a common skeletal disorder in postmenopausal women that occurs due to the simultaneous interaction of independent predisposing factors, including aging and continuous calcium loss (1). In the developed world, depending on the method of diagnosis, 9-38% of females are affected by PMOP (2). It is estimated that one-third of adult women are affected by osteoporosis-associated fractures in their lifetime, which is a public health concern (3).

The mechanism underlying all cases of osteoporosis involves an imbalance between bone resorption and formation (4). In postmenopausal women, excessive bone resorption and an inadequate rate of formation of new bone tissue are associated with estrogen deficiency (5). Low estrogen levels have been hypothesized to cause osteoporosis in women since the 1940s (6). Based on the above mechanism, various medications, including alendronate, etidronate, risedronate and strontium ranelate have been employed to prevent osteoporotic fragility fractures in patients with PMOP (7). However, the efficacy of these medications have not been directly compared and it is not clear which of these medications are the most effective (8). Furthermore, the effect of medications is not ideal; patients with PMOP need continued treatment for up to 10 years (9). It has been previously demonstrated that the peak bone mass and early menopausal bone loss are associated with the level of expression of estrogen-associated genes (10). Previous study has demonstrated that mutations in osteoclast-associated genes, including parathyroid hormone 1 receptor, colony stimulating factor 1 and low-density lipoprotein receptor-related protein 5 are associated with PMOP (11). Furthermore, bioinformatics analysis of gene expression profiles in B cells from patients with PMOP demonstrated that filamin A a and transforming growth factor-β1 may be potential target genes associated with the pathogenesis of PMOP (12). In addition, certain transcription factors (TFs), such as catenin β1, and pathways, including the mitogen-activated protein kinase signaling pathway, have been demonstrated to be involved in primary osteoporosis by DNA microarray analysis (1). Therefore, a thorough understanding of the mechanisms underlying PMOP may be based on bioinformatics analysis and may contribute to the development of novel and effective treatment approaches for PMOP.

In the present study, a bioinformatics analysis was performed based on a gene expression profile of 12 tissue

samples from ovariectomized (OVX) mice and 11 normal tissue samples from sham surgery mice. Differentially expressed gene (DEG) investigation, function and pathway enrichment studies, as well as protein-protein interaction network (PPI) analyses, were performed. Furthermore, TF-target gene regulatory networks and chemical-gene interaction networks were investigated. The present study aimed to systematically investigate potential genes and TFs associated with the progression of PMOP, which may aid in elucidating the molecular mechanism underlying PMOP. Additionally, potential chemical compounds that may be employed for the treatment of PMOP were also identified. The present study may provide insights into PMOP that may aid the development of novel and effective therapies for PMOP.

Materials and methods

Data resource. Gene expression profile data (accession no. GSE68303) were downloaded from the Gene Expression Omnibus (GEO) database (http://www.ncbi.nlm.nih.gov/geo/) (13). This dataset was produced on a GPL6885 Illumina MouseRef-8 v2.0 expression beadchip platform (Illumina, Inc., San Diego, CA, USA). A total of 12 tissue samples from OVX mice (OVX group) and 11 normal tissue samples from sham surgery mice (control group) were included in this dataset. The OVX and sham surgical operations were conducted by Calabrese *et al* (13). Briefly, mice were anesthetized using isoflurane and surgery was performed using a dorsal approach to excise the ovaries, and the abdominal and skin incisions were subsequently closed. At 4 weeks following surgery, the uterine weights were measured to confirm successful OVX surgeries (13).

Data preprocessing and differential expression analysis. Normalization of gene expression profile data was performed using the Robust Multichip Averaging (RMA) method (14) in Affy package version 1.44.0 (15) in R (version 3.0.0; (http://bioconductor.org/biocLite.R). DEGs were identified using unpaired t-tests using the Linear Models for Microarray Data package (limma version 3.32.2; http://www.bioconductor.org/packages/release/bioc/html/limma.html) (16) by comparing gene expression values between the OVX group and the control group. Following t-tests, the Benjamini-Hochberg procedure was performed to adjust P-values. Finally, $P<0.05$ and $|\log_2$ fold change$|>0$ was selected as the threshold for identification of DEGs. A heat map was constructed using pheatmap package version 1.08 (17) in R.

PPI network construction. The Search Tool for the Retrieval of Interacting Genes/Proteins (STRING; version 10.0; http://www.string-db.org/) database provides comprehensive coverage and access to experimental and predicted information concerning PPIs (18). Biological General Repository for Interaction Datasets (BioGRID; version 3.4; https://wiki.thebiogrid.org/) is an open access database that contains information on genetic and protein interactions obtained from primary biomedical literature for numerous model organisms and humans (19). Mentha (http://mentha.uniroma2.it/about.php) is a resource used to browse integrated protein-interaction networks (20). Furthermore, the Human Protein Reference Database (HPRD; release no. 9; www.hprd.org/) is a centralized platform for the visual representation and integration of information pertaining to domain architecture, post-translational modifications, interaction networks and disease association for each protein in the human proteome (21). In the present study, these four databases were used to predict PPIs.

Based on the above databases, a PPI network was constructed using upregulated and downregulated DEGs, and visualized using Cytoscape software (version 3.2.0) (22). Topological index of a network (degree centrality) is defined as the number of links incident upon a node (23). The score of each node was determined by degree centrality, where an increased score indicates a more important location within the network.

Investigation of modules in the PPI network. It has been previously demonstrated that genes from the same module in a PPI network serve similar roles and are implicated in the same biological functions (24). Analysis of modules in PPI networks was performed using ClusterONE package in Cytoscape software (22) using the cut-off value of $P<0.001$.

Enrichment analysis of the DEGs. Multifaceted Analysis Tool for Human Transcriptome (MATHT, http://www.biocloudservice.com) is an online tool that provides a comprehensive set of functional annotation tools for investigators to understand the biological roles served by large lists of genes. Gene Ontology (GO, http://www.geneontology.org/) provides structured, controlled vocabulary and classification that includes several domains of molecular and cellular biology, and is available for the scientific community to annotate genes, gene products and sequences (25). Furthermore, Kyoto Encyclopedia of Genes and Genomes (KEGG) is a knowledge base for the systematic analysis of gene functions in terms of networks of genes and molecules (26). In the present study, GO-Biological Process (GO-BP) function and KEGG pathway enrichment analyses of DEGs were performed utilizing the MATHT based on Fisher's method. $P<0.05$ was considered to indicate a statistically significant difference.

TF-target gene regulatory network construction. The regulation of gene expression by TFs is important. Analysis of TF binding sites is required for the investigation of gene regulation systems. In the present study, a transcriptional regulatory network was constructed based on the Overrepresentation Enrichment Analysis (ORA) method using the WebGestalt database (http://www.webgestalt.org/option.php) (8). The TF-target gene regulatory network was visualized using Cytoscape software (version 3.2.0). False discovery rate (FDR) <0.05 was considered the threshold.

Chemical-gene interaction network construction. The Comparative Toxicogenomics Database (CTD) provides manually curated information concerning chemical-gene/protein interactions, and chemical-disease and gene-disease associations (27). The interactions between chemicals and genes were determined using the CDT. Subsequently, the chemical-gene interaction network was constructed using Cytoscape software (version 3.2.0).

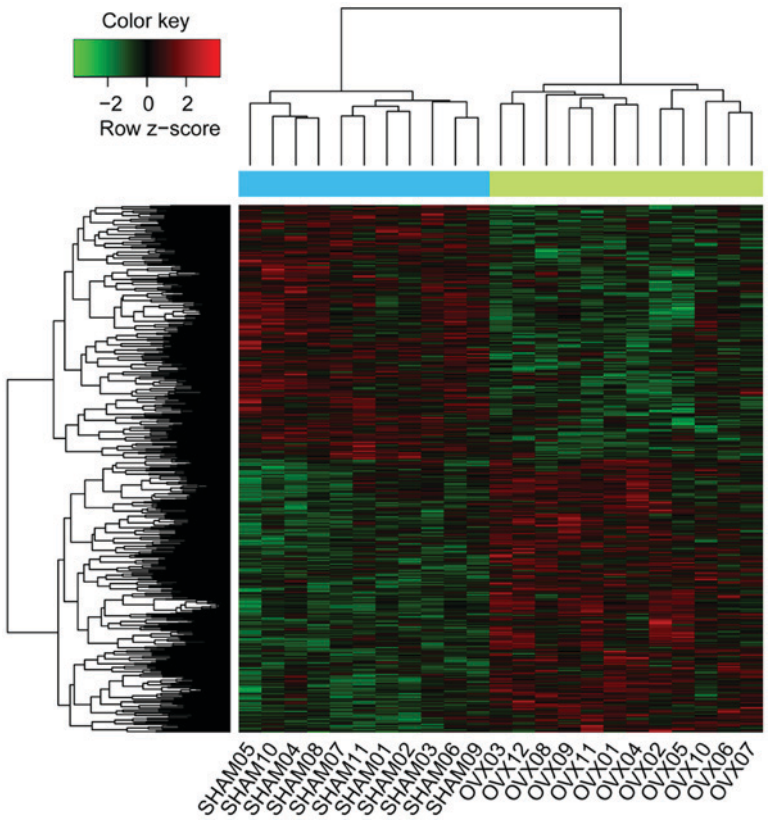

Figure 1. Heat map presenting differentially expressed genes between the ovariectomized group and control group. Red, upregulated genes; Green, downregulated genes; SHAM, control group; OVX, ovariectomized group.

Results

DEGs in OVX samples compared with control samples. As large amounts of data are included in a gene expression profile, the original data was analyzed and filtered. A total of 784 upregulated and 729 downregulated DEGs were identified. A heat map of upregulated and downregulated DEGs was constructed (Fig. 1) from DNA microarray data, reflecting the gene expression values between the control and OVX groups.

PPI network and module analysis. To identify potential interactions between DEGs, a PPI network was constructed based on protein interactions between DEGs. The results identified 552 nodes (genes) in upregulated DEGs, including protein tyrosine phosphatase receptor type C, protein tyrosine phosphatase non-receptor type 6, spleen tyrosine kinase, proto-oncogene vav, phosphatidylinositol-4,5-bisphosphate 3-kinase catalytic subunit γ isoform and γ-actin 11. In addition, 493 nodes were identified in downregulated DEGs, including polo-like kinase 1, cell division cycle 6 (CDC6), minichromosome maintenance complex component (MCM)3, ribonucleoside-diphosphate reductase subunit M2, MCM7 and baculoviral inhibitor of apoptosis repeat-containing 5 (BIRC5; data not shown).

A total of 2 upregulated and 6 downregulated modules were identified in the PPI network with P<0.001 using Cytoscape software. There were 14 nodes and 91 interactions in one of the upregulated modules (module a; $P=1.173x10^{-7}$; Fig. 2A) and 9 nodes and 27 interactions in the other upregulated module (module b; $P=5.498x10^{-4}$; Fig. 2B). The following number of nodes and interactions were observed in the 6 downregulated modules: 32 nodes and 254 interactions in module a (P=0; Fig. 3A), 31 nodes and 239 interactions in module b ($P=8.384x10^{-9}$; Fig. 3B), 13 nodes and 78 interactions in module c ($P=3.342x10^{-7}$; Fig. 3C), 13 nodes and 41 interactions in module d ($P=5.799x10^{-4}$; Fig. 3D), 12 nodes and 34 interactions in module e ($P=8.300x10^{-4}$; Fig. 3E) and 14 nodes and 36 interactions in module f ($P=9.507x10^{-4}$; Fig. 3F).

Functional enrichment analysis for DEGs. To further elucidate the roles of DEGs, GO functional and KEGG pathway enrichment analyses were performed. The upregulated DEGs were primarily involved in the 'sensory perception of smell' (GO accession no. 0007608), including olfactory receptor (OLFR)594, OLFR1247, OLFR846, OLFR218 and OLFR1389 genes, and KEGG pathway 'olfactory transduction' (entry no. mmu04740), including OLFR594, OLFR1247, OLFR846, OLFR218 and OLFR1389 genes (Table I). Furthermore, the downregulated DEGs were involved in 'DNA replication initiation' (GO accession no. 0006270), including cyclin E2, CDC6, MCM7, and origin recognition complex subunit 5 and 6 genes, 'cell cycle' (GO accession no. 0007049), including fizzy and cell division cycle 20-related 1 (FZR1), kinetochore-associated 1, BIRC5, checkpoint kinase 2 and MCM3 genes, and 'sensory perception of smell' (GO accession no. 0007608), including OLFR1249, OLFR239, OLFR177, OLFR1098 and OLFR703 genes. Downregulated DEGs were primarily involved in KEGG pathways of 'cell cycle' (entry no. mmu04110), including E2F transcription factor 1,

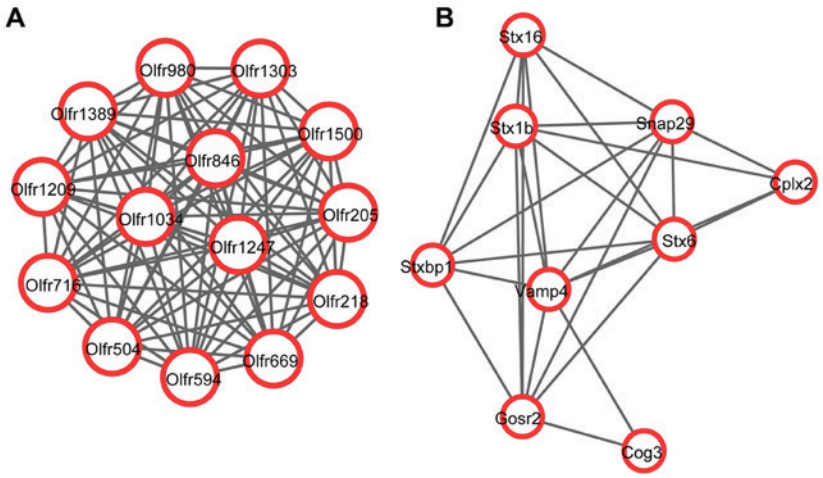

Figure 2. Two modules of upregulated differentially expressed genes. (A) Module a with 14 nodes and 91 interactions. (B) Module b with 9 nodes and 27 interactions.

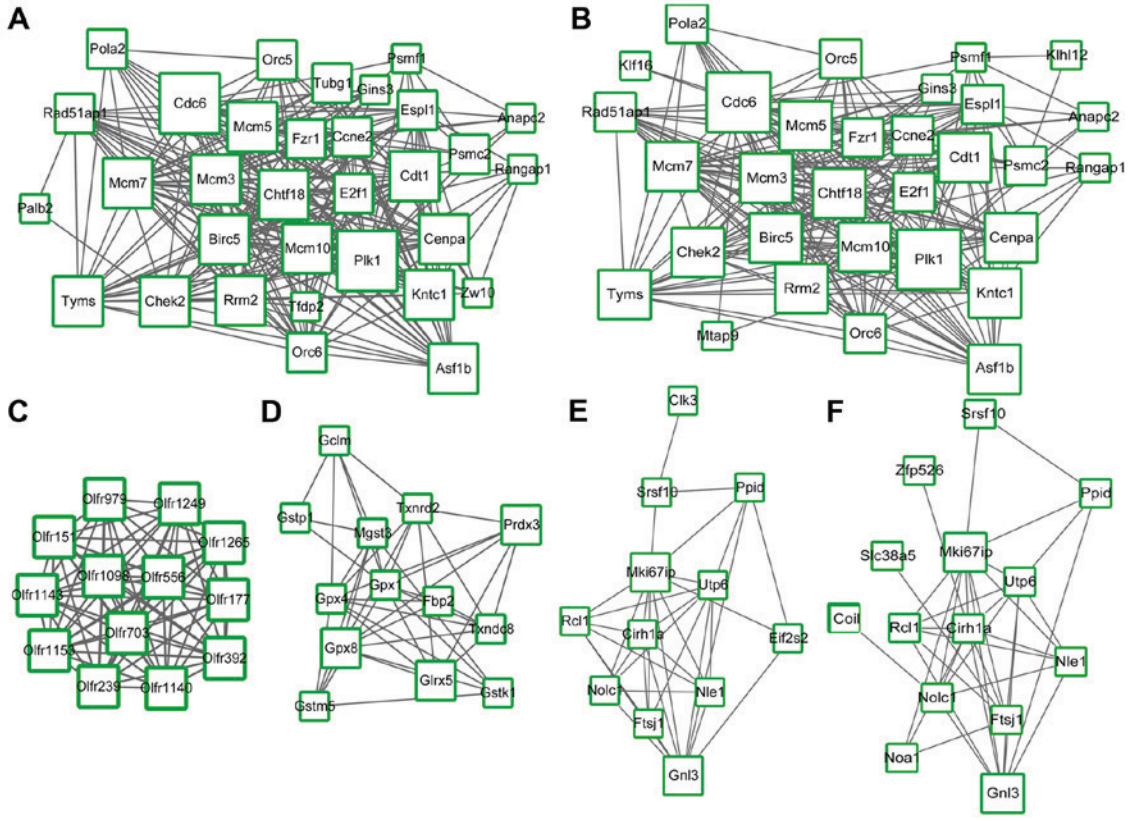

Figure 3. Six modules of downregulated differentially expressed genes. (A) Module a with 32 nodes and 254 interactions. (B) Module b with 31 nodes and 239 interactions. (C) Module c with 13 nodes and 78 interactions. (D) Module d with 13 nodes and 41 interactions. (E) Module e with 12 nodes and 34 interactions. (F) Module f with 14 nodes and 36 interactions.

anaphase-promoting complex subunit 2, CDC6, FZR1 and extra spindle pole bodies-like 1 genes, 'DNA replication' (entry no. mmu03030), including MCM7, DNA polymerase α subunit 2, MCM3 and MCM5 genes, and 'glutathione metabolism' (entry no. mmu00480), including microsomal glutathione S-transferase 3, glutathione peroxidase (GPX)1, glutathione S-transferase κ1, GPX4 and GPX8 genes. Detailed functional analyses of downregulated DEGs in 6 modules are presented in Table II.

TF-target gene regulatory network analysis. To further investigate the association between TFs and their target genes, the TF-target gene network was constructed using WebGestalt software. Using FDR<0.05 as a cut-off value, the results demonstrated that there were 187 upregulated DEGs, including high-mobility group protein, forkhead box protein P1, sodium-hydrogen antiporter 3 regulator 1 and G protein-coupled receptor kinase-interactor 2, and certain TFs, including protein ETS1, ETS-2 and other ETS family

Table I. Results of GO function and KEGG pathway enrichment analyses of upregulated differentially expressed genes in postmenopausal osteoporosis (all the significant terms or the top 5 most significant terms of the KEGG pathways or GO_BP were listed).

A, GO function and KEGG pathway enrichment analyses of DEGs in the upregulated module a

ID	Analysis type	Process	Count	P-value	Genes
mmu04740	KEGG pathway	Olfactory transduction	13	$5.33x10^{-11}$	OLFR594, OLFR1247, OLFR846, OLFR218, OLFR1389, OLFR1303, OLFR1209, OLFR980, OLFR1034, OLFR1500, OLFR716, OLFR205, OLFR669
GO: 0007608	GO_BP	Sensory perception of smell	14	$2.41x10^{-16}$	OLFR594, OLFR1247, OLFR846, OLFR218, OLFR1389, OLFR1303, OLFR1209, OLFR980, OLFR1034, OLFR1500, OLFR716, OLFR205, OLFR504, OLFR669
GO: 0007186	GO_BP	G-protein coupled receptor signaling pathway	14	$4.50x10^{-14}$	OLFR594, OLFR1247, OLFR846, OLFR218, OLFR1389, OLFR1303, OLFR1209, OLFR980, OLFR1034, OLFR1500, OLFR716, OLFR205, OLFR504, OLFR669
GO: 0050907	GO_BP	Detection of chemical stimulus involved in sensory perception	4	$3.83x10^{-4}$	OLFR1247, OLFR218, OLFR1303, OLFR1209

B, GO function and KEGG pathway enrichment analyses of DEGs in the upregulated module b

ID	Analysis type	Process	Count	P-value	Genes
mmu04130	KEGG pathway	SNARE interactions in vesicular transport	6	$2.17x10^{-11}$	SNAP29, STX6, STX16, VAMP4, GOSR2, STX1B
mmu04721	KEGG pathway	Synaptic vesicle cycle	3	$1.30x10^{-3}$	CPLX2, STXBP1, STX1B
GO: 0016192	GO_BP	Vesicle-mediated transport	6	$1.18x10^{-8}$	STX6, STX16, STXBP1, VAMP4, GOSR2, STX1B
GO: 0015031	GO_BP	Protein transport	7	$3.18x10^{-8}$	COG3, SNAP29, STX6, STX16, STXBP1, GOSR2, STX1B
GO: 0006810	GO_BP	Transport	8	$7.62x10^{-7}$	COG3, SNAP29, STX6, CPLX2, STX16, STXBP1, GOSR2, STX1B
GO: 0090161	GO_BP	Golgi ribbon formation	3	$9.40x10^{-6}$	STX6, STX16, VAMP4
GO: 0031629	GO_BP	Synaptic vesicle fusion to presynaptic active zone membrane	3	$1.55x10^{-5}$	SNAP29, STXBP1, STX1B

GO, Gene Ontology; GO_BP, GO Biological Process; KEGG, Kyoto Encyclopedia of Genes and Genomes; DEGs, differentially expressed genes.

members, GA-binding protein, myc-associated factor X, Spi-1 proto-oncogene/PU1, SP1 TF (SP1) and CDC5 in this network (Fig. 4).

Chemical-gene interaction network analysis. Based on the CTD database, the present study revealed a total of 79,334 chemical-gene interactions identified in osteoporosis patients or in postmenopausal women. Among these interactions, a total of 850 interactions were identified between upregulated genes and chemicals (375 upregulated genes and 15 chemicals; Fig. 5). There were 781 interactions between downregulated genes and chemicals (375 downregulated genes and 14 chemicals; Fig. 6). Certain chemicals, including estradiol, resveratrol, quercetin, calcitriol, genistein and raloxifene were identified as key chemicals in upregulated or downregulated DEG-chemical networks.

Table II. Results of GO function and KEGG pathway enrichment analyses of downregulated DEGs in postmenopausal osteoporosis (all the significant terms or the top 5 most significant terms of the KEGG pathways or GO_BP were listed).

A, GO function and KEGG pathway enrichment analyses of DEGs in the downregulated module a

ID	Analysis type	Process	Count	P-value	Genes
mmu04110	KEGG pathway	Cell cycle	14	4.52×10^{-19}	E2F1, ANAPC2, CDC6, FZR1, ESPL1, CHEK2, MCM3, MCM5, CCNE2, MCM7, PLK1, TFDP2, ORC5, ORC6
mmu03030	KEGG pathway	DNA replication	4	1.07×10^{-4}	MCM7, POLA2, MCM3, MCM5
mmu04114	KEGG pathway	Oocyte meiosis	4	3.11×10^{-3}	CCNE2, ANAPC2, PLK1, ESPL1
mmu04115	KEGG pathway	P53 signaling pathway	3	1.40×10^{-2}	CCNE2, RRM2, CHEK2
mmu04914	KEGG pathway	Progesterone-mediated oocyte maturation	3	2.29×10^{-2}	ANAPC2, FZR1, PLK1
GO: 0006270	GO_BP	DNA replication initiation	9	2.01×10^{-17}	CCNE2, CDC6, MCM7, ORC5, ORC6, POLA2, MCM3, MCM10, MCM5
GO: 0006260	GO_BP	DNA replication	12	6.83×10^{-17}	CDC6, MCM7, GINS3, RRM2, CHTF18, ORC5, ORC6, POLA2, MCM3, MCM10, MCM5, CDT1
GO: 0007049	GO_BP	Cell cycle	16	1.41×10^{-14}	E2F1, ANAPC2, CDC6, FZR1, KNTC1, BIRC5, CHEK2, MCM3, MCM5, CDT1, CCNE2, MCM7, PLK1, TFDP2, CHTF18, ZW10
GO: 0051301	GO_BP	Cell division	10	8.49×10^{-9}	CCNE2, ANAPC2, CDC6, FZR1, PLK1, BIRC5, CHEK2, KNTC1, MCM5, ZW10
GO: 0007067	GO_BP	Mitotic nuclear division	9	1.59×10^{-8}	ANAPC2, CDC6, FZR1, PLK1, KNTC1, BIRC5, ESPL1, CHEK2, ZW10

B, GO function and KEGG pathway enrichment analyses of DEGs in the downregulated module b

ID	Analysis type	Process	Count	P-value	Genes
mmu04110	KEGG pathway	Cell cycle	13	7.81×10^{-18}	CCNE2, E2F1, ANAPC2, CDC6, FZR1, MCM7, PLK1, ORC5, ORC6, ESPL1, CHEK2, MCM3, MCM5
mmu03030	KEGG pathway	DNA replication	4	7.87×10^{-5}	MCM7, POLA2, MCM3, MCM5
mmu04114	KEGG pathway	Oocyte meiosis	4	2.31×10^{-3}	CCNE2, ANAPC2, PLK1, ESPL1
mmu04115	KEGG pathway	P53 signaling pathway	3	1.15×10^{-2}	CCNE2, RRM2, CHEK2
mmu04914	KEGG pathway	Progesterone-mediated oocyte maturation	3	1.90×10^{-2}	CCNE2, RRM2, CHEK2
GO: 0006270	GO_BP	DNA replication initiation	9	1.09×10^{-17}	CCNE2, CDC6, MCM7, ORC5, ORC6, POLA2, MCM3, MCM10, MCM5
GO: 0006260	GO_BP	DNA replication	12	2.82×10^{-17}	CDC6, MCM7, GINS3, RRM2, CHTF18, ORC5, ORC6, POLA2, MM3,C MCM10, MCM5, CDT1
GO: 0007049	GO_BP	Cell cycle	14	2.90×10^{-12}	CCNE2, E2F1, ANAPC2, CDC6, FZR1, MCM7, PLK1, KNTC1, CHTF18, BIRC5, CHEK2, MCM3, MCM5, CDT1
GO: 0051301	GO_BP	Cell division	9	9.13×10^{-8}	CCNE2, ANAPC2, CDC6, FZR1, PLK1, KNTC1, BIRC5, CHEK2, MCM5
GO: 0007067	GO_BP	Mitotic nuclear division	8	2.15×10^{-7}	ANAPC2, CDC6, FZR1, PLK1, KNTC1, BIRC5, ESPL1, CHEK2

Table II. Continued.

C, GO function and KEGG pathway enrichment analyses of DEGs in the downregulated module c

ID	Analysis type	Process	Count	P-value	Genes
mmu04740	KEGG pathway	Olfactory transduction	12	$3.84x10^{-10}$	OLFR239, OLFR177, OLFR1143, OLFR556, OLFR1098, OLFR703, OLFR1265, OLFR151, OLFR392, OLFR979, OLFR1140, OLFR1153
GO: 0007608	GO_BP	Sensory perception of smell	13	$3.85x10^{-15}$	OLFR1249, OLFR239, OLFR177, OLFR1098, OLFR703, OLFR1265, OLFR151, OLFR1143, OLFR556, OLFR392, OLFR1153, OLFR1140, OLFR979
GO:0007186	GO_BP	G-protein coupled receptor signaling pathway	13	$4.80x10^{-13}$	OLFR1249, OLFR239, OLFR177, OLFR1098, OLFR703, OLFR1265, OLFR151, OLFR1143, OLFR556, OLFR392, OLFR1153, OLFR1140, OLFR979

D, GO function and KEGG pathway enrichment analyses of DEGs in the downregulated module d

ID	Analysis type	Process	Count	P-value	Genes
mmu00480	KEGG pathway	Glutathione metabolism	8	$2.23x10^{-14}$	MGST3, GPX1, GSTK1, GPX4, GPX8, GCLM, GSTM5, GSTP1
mmu00980	KEGG pathway	Metabolism of xenobiotics by cytochrome P450	4	$4.41x10^{-5}$	MGST3, GSTK1, GSTM5, GSTP1
mmu00982	KEGG pathway	Drug metabolism-cytochrome P450	4	$4.83x10^{-5}$	MGST3, GSTK1, GSTM5, GSTP1
mmu05204	KEGG pathway	Chemical carcinogenesis	4	$1.31x10^{-4}$	MGST3, GSTK1, GSTM5, GSTP1
GO: 0006749	GO_BP	Glutathione metabolic process	6	$9.25x10^{-11}$	GPX1, GSTK1, GPX4, GCLM, GSTM5, GSTP1
GO: 0045454	GO_BP	Cell redox homeostasis	5	$7.37x10^{-8}$	GPX1, GLRX5, TXNDC8, TXNRD2, PRDX3
GO: 0006979	GO_BP	Response to oxidative stress	5	$1.32x10^{-6}$	GPX1, GPX4, GPX8, PRDX3, GCLM
GO: 0055114	GO_BP	Oxidation-reduction process	6	$4.58x10^{-5}$	GPX1, TXNDC8, GPX4, TXNRD2, GPX8, PRDX3
GO: 0042744	GO_BP	Hydrogen peroxide catabolic process	2	$9.25x10^{-3}$	GPX1, PRDX3

E, GO function and KEGG pathway enrichment analyses of DEGs in the downregulated module e

ID	Analysis type	Process	Count	P-value	Genes
mmu03008	KEGG pathway	Ribosome biogenesis in eukaryotes	4	$1.18x10^{-5}$	RCL1, UTP6, CIRH1A, GNL3
GO: 0006364	GO_BP	rRNA processing	3	$2.09x10^{-3}$	RCL1, UTP6, CIRH1A
GO: 0006396	GO_BP	RNA processing	2	$3.97x10^{-2}$	RCL1, UTP6
GO: 0042254	GO_BP	Ribosome biogenesis	2	$4.82x10^{-2}$	RCL1, UTP6

F, GO function and KEGG pathway enrichment analyses of DEGs in the downregulated module f

ID	Analysis type	Process	Count	P-value	Genes
mmu03008	KEGG pathway	Ribosome biogenesis in eukaryotes	4	$1.18x10^{-5}$	RCL1, UTP6, CIRH1A, GNL3

Table II. Continued.

F, GO function and KEGG pathway enrichment analyses of DEGs in the downregulated module f

ID	Analysis type	Process	Count	P-value	Genes
GO: 0042254	GO_BP	Ribosome biogenesis	3	$1.28x10^{-3}$	RCL1, NOA1, GNL3
GO: 0006364	GO_BP	rRNA processing	3	$2.54x10^{-3}$	RCL1, UTP6, CIRH1A
GO: 0006396	GO_BP	RNA processing	2	$4.35x10^{-2}$	RCL1, UTP6

GO, Gene Ontology; GO_BP, GO Biological Process; KEGG, Kyoto Encyclopedia of Genes and Genomes; DEGs, differentially expressed genes.

Figure 4. Transcription factor-target gene regulatory network. Blue hexagon represents a transcription factor, red circle represents an upregulated gene, arrows indicate the direction of regulation.

Discussion

PMOP, frequently associated with skeletal disorders among elderly women, represents a medical and economic burden (1). It has been demonstrated that estrogen serves a role in the regulation of bone turnover (5,28). However, the role of estrogen deficiency in the mechanisms underlying PMOP based on gene expression patterns has not been previously investigated.

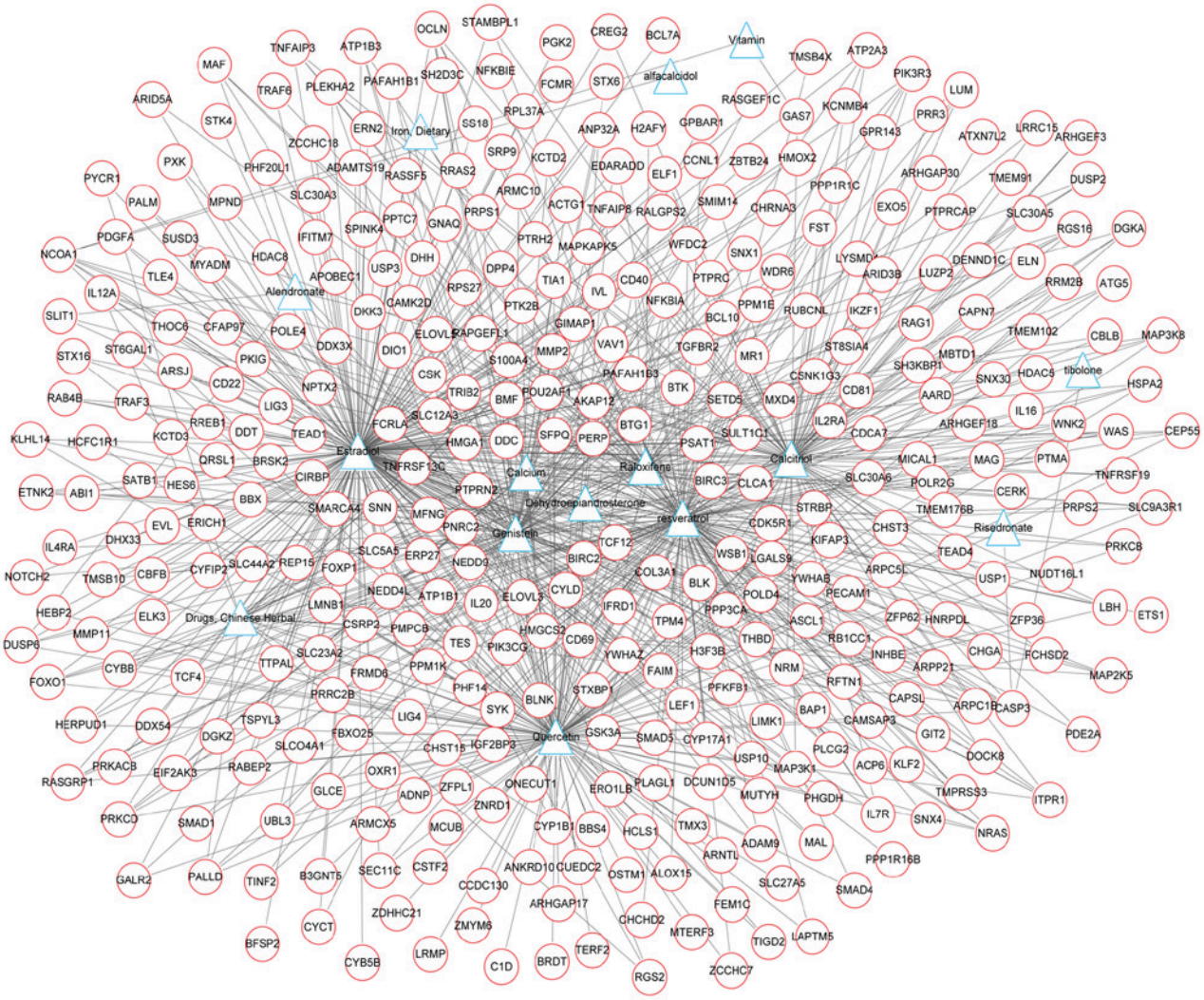

Figure 5. Upregulated gene-chemical interaction network. Red circle represents the upregulated gene, blue triangle represents a chemical.

In the present study, the upregulated DEGs in modules were enriched in 'sensory perception of smell' function and 'olfactory transduction' pathway. OLFR family genes were enriched in the upregulated modules. Downregulated DEGs in modules were enriched in 'DNA replication initiation' function and 'cell cycle' pathway. A total of 8 TFs, including SP1 and ETS1, were associated with PMOP. Furthermore, estradiol and resveratrol were key chemicals in the chemical-gene interaction network.

Estrogen has an important role in bone metabolism/remodeling, and estrogen deficiency leads to bone loss, as identified in maxillary alveolar bone (29). Therefore, the reduced estrogen levels in post-menopausal women may influence the progression of bone formation (29). Bone morphogenetic proteins (BMPs) serve roles in the process of bone formation and maintenance (30). Shou *et al* (31) indicated that the survival of OLFR neurons was regulated by BMPs *in vitro*. OFLR family genes, which are expressed in the cell membranes of OFLR neurons, are members of the class A rhodopsin-like family of G protein-coupled receptors (32). Wineland *et al* (33) demonstrated that the regulation of BMP levels was crucial to the development and maintenance of OLFR neurons and that overexpression of BMPs led to reduced numbers of OLFR neurons. In the present study, 'sensory perception of smell' and 'olfactory transduction' were the most enriched GO functions and KEGG pathways for upregulated DEGs, respectively. The upregulated DEGs that were associated with the most enriched function and pathway all belonged to the OLFR family and included OLFR846, OLFR218 and OLFR1389 genes, which suggests that the OLFR family may serve an important role in the process of PMOP. Therefore, based on the above results, it may be hypothesized that estrogen deficiency may induce low expression of BMPs, which further leads to the overexpression of OLFR genes. However, researching concerning the association between estrogen, the OLFR family and bone development has been neglected in recent years, and further investigation is necessary to confirm the pathological mechanism underlying PMOP. Furthermore, 50 years ago, estrogen was reported to alter the duration of DNA synthesis and the cell cycle in mice (34). Recently, Javanmoghadam *et al* (35) indicated that estrogen receptor α regulated the cell cycle in a ligand-dependent manner. In the present study, downregulated DEGs were primarily enriched in 'DNA replication initiation' function and 'cell cycle' pathway. These results indicate that estrogen deficiency may lead to the reduced expression of genes enriched in 'DNA replication initiation' and 'cell cycle'

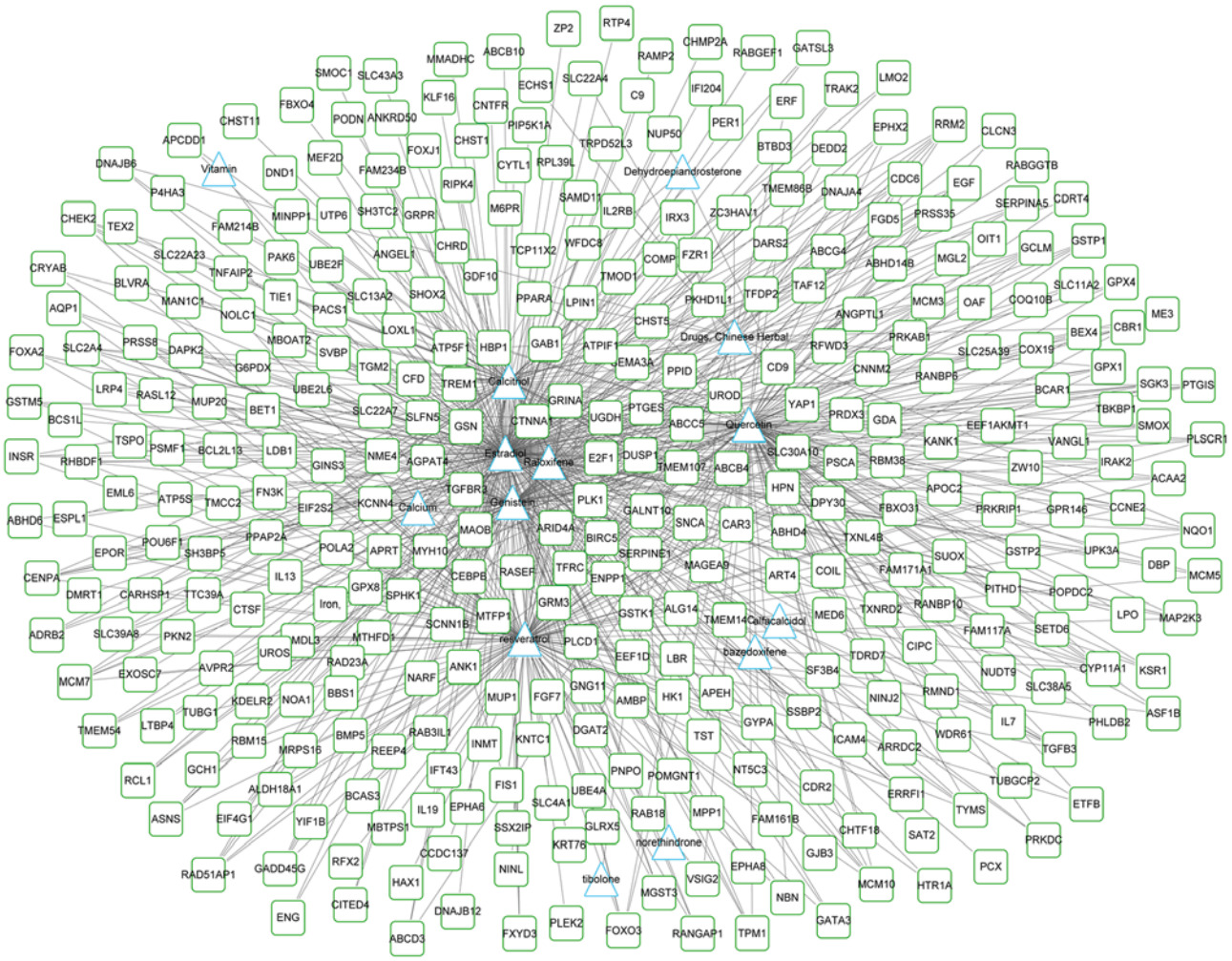

Figure 6. Downregulated gene-chemical interaction network. Green square represents a downregulated gene, blue triangle represents a chemical.

functions and pathways, respectively, which may further influence the process of bone formation.

SP1 is a protein encoded by the SP1 gene in humans (36). SP1 functions as an osteogenic cell fate-determining factor by regulating gene expression at the transcriptional level (37). Based on a DNA microarray analysis, Xie *et al* (11) demonstrated that SP1 regulated the majority of upregulated DEGs from primary osteoporosis tissue samples and normal bone tissue samples. Furthermore, a large-scale gene analysis demonstrated that SP1 polymorphism was associated with reduced bone mineral density and may predispose females to incident vertebral fractures (38). ETS1, which is a member of the ETS family of transcription factors, is a protein encoded by the ETS1 gene in humans (39). Ring finger protein 11 is expressed in bone cells during osteogenesis and is regulated by ETS1 (40). Almeida *et al* (41) indicated that in bone stromal cell-derived lesions, protein kinase A regulates caspase 1 via ETS1. In a tissue engineering study, Sutter *et al* (42) revealed differential expression of ETS2 in tissue engineered bone constructs *in vitro*, demonstrating an association between ETS2 and osteogenesis. However, direct evidence of associations between these genes and PMOP is rare. In the present study, SP1, ETS1 and ETS2 were identified as key TFs in the TF-target gene network, which further indicated that these TFs may serve roles in the process of PMOP. The identification of the enriched TFs may improve the understanding of the mechanisms underlying PMOP.

Furthermore, several chemicals, including estradiol and resveratrol, were identified in the present study. Estradiol is a medication and a naturally occurring steroid hormone (43). Estradiol is used in hormone replacement therapies for the treatment of moderate to severe menopausal symptoms, including osteoporosis (44). Resveratrol is a polyphenolic phytoalexin that also exhibits osteoprotective and chondroprotective properties (45). Preclinical evidence from rat models of osteoporosis demonstrated that resveratrol may be used as a therapeutic agent for bone loss (46). A recent study demonstrated that oral gavage of rats with resveratrol at 1 mg/kg/day may potentially prevent bone defects (47). Therefore, these chemicals identified in the present study may be used for treatment of PMOP in the future.

However, certain limitations are associated with the present study. No animal, molecular or cellular biological experiments were conducted in the present study. The microarray data was generated by research by Calabrese *et al* (13), but whether the OVX and sham surgical operations were performed under identical conditions is not known.

In conclusion, functions, including 'sensory perception of smell' and 'DNA replication initiation', as well as pathways, including 'olfactory transduction' and 'cell cycle', may serve

roles in the process of PMOP. Furthermore, the OLFR family genes, and SP1 and ETS1 TFs, may be involved in the progression of PMOP. Additionally, chemicals, including estradiol and resveratrol, may in the future be used for the treatment of PMOP. The results of the present study should be further confirmed by a study with a larger sample size, and by *in vitro* and *in vivo* experiments. A greater number of potential molecular pathways and genes underlying the progress of PMOP should be identified.

References

1. Black DM and Rosen CJ: Clinical practice. Postmenopausal osteoporosis. N Engl J Med 374: 254-262, 2016.
2. Wade SW, Strader C, Fitzpatrick LA, Anthony MS and O'Malley CD: Estimating prevalence of osteoporosis: Examples from industrialized countries. Arch Osteoporos 9: 182, 2014.
3. Kwun S, Laufgraben ML and Gopalakrishnan G: Prevention and treatment of postmenopausal osteoporosis. The Obstetrician & Gynaecologist 14: 251-256, 2012.
4. Ralston SH: The genetics of osteoporosis. Br Med Bull 90: 247, 2015.
5. Heiss C, Govindarajan P, Schlewitz G, Hemdan NY, Schliefke N, Alt V, Thormann U, Lips KS, Wenisch S, Langheinrich AC, *et al*: Induction of osteoporosis with its influence on osteoporotic determinants and their interrelationships in rats by DEXA. Med Sci Monit 18: BR199-BR207, 2012.
6. Kenigsberg D and Hull ME: Bone calcium dynamics in women with declining estrogen levels. Springer Netherlands: 153-160, 1990.
7. Eastell R: Prevention and management of osteoporosis. Medicine 45: 565-569, 2017.
8. Body JJ: How to manage postmenopausal osteoporosis? Acta Clin Belg 66: 443-447, 2011.
9. Adler RA, El-Hajj Fuleihan G, Bauer DC, Camacho PM, Clarke BL, Clines GA, Compston JE, Drake MT, Edwards BJ, Favus MJ, *et al*: Managing osteoporosis in patients on Long-term bisphosphonate treatment: Report of a task force of the American society for bone and mineral research. J Bone Miner Res 31: 1910, 2016.
10. Keen RW, Woodford-Richens KL, Lanchbury JS and Spector TD: Peak bone mass, early menopausal bone loss and polymorphism at the oestrogen receptor gene. Osteoporosis Int 6: 102, 1996.
11. Xie W, Ji L, Zhao T and Gao P: Identification of transcriptional factors and key genes in primary osteoporosis by DNA microarray. Med Sci Monit 21: 1333-1344, 2015.
12. Ma M, Luo S, Zhou W, Lu L, Cai J, Yuan F and Yin F: Bioinformatics analysis of gene expression profiles in B cells of postmenopausal osteoporosis patients. Taiwan J Obstet Gynecol 56: 165-170, 2017.
13. Calabrese G, Mesner LD, Foley PL, Rosen CJ and Farber CR: Network analysis implicates alpha-synuclein (Snca) in the regulation of Ovariectomy-induced bone loss. Sci Rep 6: 29475, 2016.
14. Irizarry RA, Hobbs B, Collin F, Beazer-Barclay YD, Antonellis KJ, Scherf U and Speed TP: Exploration, normalization, and summaries of high density oligonucleotide array probe level data. Biostatistics 4: 249-264, 2003.
15. Gautier L, Cope L, Bolstad BM and Irizarry RA: Affy-analysis of Affymetrix GeneChip data at the probe level. Bioinformatics 20: 307-315, 2004.
16. Diboun I, Wernisch L, Orengo CA and Koltzenburg M: Microarray analysis after RNA amplification can detect pronounced differences in gene expression using limma. BMC Genomics 7: 252, 2006.
17. Wang L, Cao C, Ma Q, Zeng Q, Wang H, Cheng Z, Zhu G, Qi J, Ma H, Nian H and Wang Y: RNA-seq analyses of multiple meristems of soybean: Novel and alternative transcripts, evolutionary and functional implications. BMC Plant Biol 14: 169, 2014.
18. Szklarczyk D, Franceschini A, Kuhn M, Simonovic M, Roth A, Minguez P, Doerks T, Stark M, Muller J, Bork P, *et al*: The STRING database in 2011: Functional interaction networks of proteins, globally integrated and scored. Nucleic Acids Res 39 (Database Issue): D561-D568, 2011.
19. Chatr-Aryamontri A, Breitkreutz BJ, Oughtred R, Boucher L, Heinicke S, Chen D, Stark C, Breitkreutz A, Kolas N, O'Donnell L, *et al*: The BioGRID interaction database: 2015 update. Nucleic Acids Res 43 (Database Issue): D470-D478, 2015.
20. Calderone A, Castagnoli L and Cesareni G: Mentha: A resource for browsing integrated protein-interaction networks. Nat Methods 10: 690-691, 2013.
21. Liu B and Hu B: HPRD: A High performance RDF database. Springer Berlin Heidelberg, pp364-374, 2007.
22. Shannon P, Markiel A, Ozier O, Baliga NS, Wang JT, Ramage D, Amin N, Schwikowski B and Ideker T: Cytoscape: A software environment for integrated models of biomolecular interaction networks. Genome Res 13: 2498-2504, 2003.
23. Sharma D and Surolia A: Degree Centrality. In: Encyclopedia of Systems Biology. Dubitzky W, Wolkenhauer O, Cho KH and Yokota H (eds.) Springer New York, New York, NY, pp558-558, 2013.
24. Wang J, Ren J, Li M and Wu FX: Identification of hierarchical and overlapping functional modules in PPI networks. IEEE Trans Nanobioscience 11: 386-393, 2012.
25. Gene Ontology Consortium: The gene ontology (GO) project in 2006. Nucleic Acids Res 34 (Database Issue): D322-D326, 2006.
26. Ogata H, Goto S, Sato K, Fujibuchi W, Bono H and Kanehisa M: KEGG: Kyoto encyclopedia of genes and genomes. Nucleic Acids Res 27: 29-34, 1999.
27. Davis AP, Grondin CJ, Lennon-Hopkins K, Saraceni-Richards C, Sciaky D, King BL, Wiegers TC and Mattingly CJ: The comparative toxicogenomics database's 10th year anniversary: Update 2015. Nucleic Acids Res 43 (Database Issue): D914-D920, 2015.
28. Verbruggen SW, Vaughan TJ and Mcnamara LM: Mechanisms of osteocyte stimulation in osteoporosis. J Mech Behav Biomed Mater 62: 158-168, 2016.
29. Xu XC, Chen H, Zhang X, Zhai ZJ, Liu XQ, Zheng XY, Zhang J, Qin A and Lu EY: Effects of oestrogen deficiency on the alveolar bone of rats with experimental periodontitis. Mol Med Rep 12: 3494-3502, 2015.
30. Katagiri T and Watabe T: Bone morphogenetic proteins. Cold Spring Harb Perspect Biol 8: pii:a021899, 2016.
31. Shou J, Murray RC, Rim PC and Calof AL: Opposing effects of bone morphogenetic proteins on neuron production and survival in the olfactory receptor neuron lineage. Development 127: 5403-5413, 2000.
32. Hussain A, Saraiva LR and Korsching SI: Positive Darwinian selection and the birth of an olfactory receptor clade in teleosts. Proc Natl Acad Sci USA 106: 4313-4318, 2009.
33. Wineland A, Blitz IL, Murray RC and Calof AL: A transgenic approach for determining the role of bone morphogenetic proteins in the development of olfactory receptor neurons. Developmental Biol 271, 2004.
34. Galand P, Rodesch F, Leroy F and Chretien J: Altered duration of DNA synthesis and cell cycle in non-target tissues of mice treated with oestrogen. Nature 216: 1211-1212, 1967.
35. Javanmoghadam S, Zhang W, Hunt KK and Keyomarsi K: Estrogen receptor alpha is cell cycle-regulated and regulates the cell cycle in a ligand-dependent fashion. Cell Cycle 15: 1579-1590, 2016.
36. Surhone LM, Tennoe MT and Henssonow SF: Sp1 Transcription Factor. Betascript Publishing2016.
37. Zhang Y, Hassan MQ, Xie RL, Hawse JR, Spelsberg TC, Montecino M, Stein JL, Lian JB, van Wijnen AJ and Stein GS: Co-stimulation of the bone-related Runx2 P1 promoter in mesenchymal cells by SP1 and ETS transcription factors at polymorphic purine-rich DNA sequences (Y-repeats). J Biol Chem 284: 3125-3135, 2009.
38. Ralston SH, Uitterlinden AG, Brandi ML, Balcells S, Langdahl BL, Lips P, Lorenc R, Obermayer-Pietsch B, Scollen S, Bustamante M, *et al*: Large-scale evidence for the effect of the COLIA1 Sp1 polymorphism on osteoporosis outcomes: The GENOMOS study. PLoS Med 3: e90, 2006.
39. Dwyer J, Li H, Xu D and Liu JP: Transcriptional regulation of telomerase activity: Roles of the the Ets transcription factor family. Ann N Y Acad Sci 1114: 36-47, 2007.
40. Gao Y, Ganss BW, Wang H, Kitching RE and Seth A: The RING finger protein RNF11 is expressed in bone cells during osteogenesis and is regulated by Ets1. Exp Cell Res 304: 127-135, 2005.

41. Almeida MQ, Tsang KM, Cheadle C, Watkins T, Grivel JC, Nesterova M, Goldbach-Mansky R and Stratakis CA: Protein kinase A regulates caspase-1 via Ets-1 in bone stromal cell-derived lesions: A link between cyclic AMP and pro-inflammatory pathways in osteoblast progenitors. Hum Mol Genet 20: 165-175, 2011.
42. Sutter W, Stein E, Koehn J, Schmidl C, Lezaic V, Ewers R and Turhani D: Effect of different biomaterials on the expression pattern of the transcription factor Ets2 in bone-like constructs. J Craniomaxillofac Surg 37: 263-271, 2009.
43. Kuhl H: Pharmacology of estrogens and progestogens: Influence of different routes of administration. Climacteric 8 (Suppl 1): S3-S63, 2005.
44. Klein-Nulend J, van Oers RF, Bakker AD and Bacabac RG: Bone cell mechanosensitivity, estrogen deficiency, and osteoporosis. J Biomech 48: 855-865, 2015.
45. Cooley J, Broderick TL, Al-Nakkash L and Plochocki JH: Effects of resveratrol treatment on bone and cartilage in obese diabetic mice. J Diabetes Metab Disord 14: 10, 2015.
46. Tou JC: Evaluating resveratrol as a therapeutic bone agent: Preclinical evidence from rat models of osteoporosis. Ann N Y Acad Sci 1348: 75-85, 2015.
47. Lee AM, Shandala T, Soo PP, Su YW, King TJ, Chen KM, Howe PR and Xian CJ: Effects of resveratrol supplementation on methotrexate Chemotherapy-induced Bone Loss. Nutrients 9: pii:E255, 2017.